Year: 2023

Blood Oxygenation Level-Dependent Cerebrovascular Reactivity-Derived Steal Phenomenon May Indicate Tissue Reperfusion Failure After Successful Endovascular Thrombectomy

Bellomo, Jacopo ; Sebök, Martina ; Stumpo, Vittorio ; van Niftrik, Christiaan H B ; Meisterhans, Darja ; Piccirelli, Marco ; Michels, Lars ; Reolon, Beno ; Esposito, Giuseppe ; Schubert, Tilman ; Kulcsar, Zsolt ; Luft, Andreas R ; Wegener, Susanne ; Regli, Luca ; Fierstra, Jorn

RESEARCH

Blood Oxygenation Level–Dependent Cerebrovascular Reactivity–Derived Steal Phenomenon May Indicate Tissue Reperfusion Failure After Successful Endovascular Thrombectomy

Jacopo Bellomo[1,2] · Martina Sebök[1,2] · Vittorio Stumpo[1,2] · Christiaan H. B. van Niftrik[1,2] · Darja Meisterhans[1,2] · Marco Piccirelli[2,3] · Lars Michels[2,3] · Beno Reolon[2,3] · Giuseppe Esposito[1,2] · Tilman Schubert[2,3] · Zsolt Kulcsar[2,3] · Andreas R. Luft[2,4,5] · Susanne Wegener[2,4] · Luca Regli[1,2] · Jorn Fierstra[1,2]

Abstract

In acute ischemic stroke due to large-vessel occlusion (LVO), the clinical outcome after endovascular thrombectomy (EVT) is influenced by the extent of autoregulatory hemodynamic impairment, which can be derived from blood oxygenation level–dependent cerebrovascular reactivity (BOLD-CVR). BOLD-CVR imaging identifies brain areas influenced by hemodynamic steal. We sought to investigate the presence of steal phenomenon and its relationship to DWI lesions and clinical deficit in the acute phase of ischemic stroke following successful vessel recanalization.

From the prospective longitudinal IMPreST (Interplay of Microcirculation and Plasticity after ischemic Stroke) cohort study, patients with acute ischemic unilateral LVO stroke of the anterior circulation with successful endovascular thrombectomy (EVT; mTICI scale $\geq$ 2b) and subsequent BOLD-CVR examination were included for this analysis. We analyzed the spatial correlation between brain areas exhibiting BOLD-CVR-associated steal phenomenon and DWI infarct lesion as well as the relationship between steal phenomenon and NIHSS score at hospital discharge.

Included patients ($n = 21$) exhibited steal phenomenon to different extents, whereas there was only a partial spatial overlap with the DWI lesion (median 19%; IQR, 8–59). The volume of steal phenomenon outside the DWI lesion showed a positive correlation with overall DWI lesion volume and was a significant predictor for the NIHSS score at hospital discharge. Patients with acute ischemic unilateral LVO stroke exhibited hemodynamic steal identified by BOLD-CVR after successful EVT. Steal volume was associated with DWI infarct lesion size and with poor clinical outcome at hospital discharge. BOLD-CVR may further aid in better understanding persisting hemodynamic impairment following reperfusion therapy.

Keywords Ischemic stroke · Large-vessel occlusion · Cerebrovascular reactivity · Steal phenomenon · BOLD-CVR · DWI · Endovascular thrombectomy · Reperfusion failure

Abbreviations

LVO	Large-vessel occlusion
BOLD	Blood oxygen level-dependent
MRI	Magnetic resonance imaging
CVR	Cerebrovascular reactivity
DWI	Diffusion-weighted imaging
EVT	Endovascular thrombectomy
NIHSS	National Institutes of Health Stroke Scale
mTICI	Modified Thrombolysis In Cerebral Infarction
IMPreST	Interplay of Microcirculation and Plasticity after ischemic Stroke
SD	Standard deviation
SE	Standard error

✉ Jacopo Bellomo
jacopo.bellomo@usz.ch

1   Department of Neurosurgery, University Hospital Zurich, Frauenklinikstrasse 10, CH-8091 Zurich, Switzerland

2   Clinical Neuroscience Center, University of Zurich and Swiss Federal Institute of Technology Zurich, Zurich, Switzerland

3   Department of Neuroradiology, University Hospital Zurich, Zurich, Switzerland

4   Department of Neurology, University Hospital Zurich, Zurich, Switzerland

5   Cereneo Center for Neurology and Rehabilitation, Vitznau, Switzerland

🖄 Springer

Introduction

Acute ischemic large-vessel occlusion (LVO) stroke is characterized by proximal occlusion of a large cerebral vessel (e.g., internal carotid artery or middle cerebral artery) and has a profound hemodynamic impact on distal brain tissue, i.e., hypoperfusion and tissue ischemia. [1] Hypoperfusion and consecutive tissue damage is a dynamic process in the acute ischemic phase which is influenced by collateral recruitment and autoregulation [1–4]. Timely restoration of cerebral blood flow by endovascular thrombectomy (EVT) is the most effective maneuver for salvaging ischemic brain tissue that is not already irreversibly lost [5–8]. However, in some cases, no improvement or even worsening of clinical status despite successful vessel recanalization can be observed. It is hypothesized that the mechanisms underlying this reperfusion failure are attributable to remaining macro- and/or microvascular dysfunction and subsequent persisting hemodynamic impairment within the ischemic territory [9–11].

In recent years, several neuroimaging techniques have been employed investigating microvasculature and hemodynamic tissue responses following acute ischemia and subsequent endovascular revascularization to predict tissue fate [10, 12, 13]. Hyper- and hypoperfusion tissue status observed with perfusion-weighted magnetic resonance imaging (MRI) have been both associated with poor clinical outcome. For instance, hypoperfusion despite successful EVT is thought to result from insufficient capillary reflow induced by different mechanisms (e.g. microvascular occlusion with microclots or neutrophils) [13–16]. Hyperperfusion, most likely, comes from persisting altered cerebrovascular autoregulation [13, 17]. A better characterization of hemodynamic tissue state in these patients would help to further understand the mechanisms underlying reperfusion failure.

Blood oxygenation-level dependent cerebrovascular reactivity (BOLD-CVR) may be suited as an emerging, clinically applicable, hemodynamic imaging technique capable to evaluate vessel reactivity and remaining vasodilatory reserve as the result of flow redistribution under a controlled hypercapnic challenge [18–20]. Of particular interest are brain areas exhibiting BOLD-CVR-associated steal phenomenon in the post-reperfusion period, indicating persisting severely impaired cerebrovascular autoregulatory loss [21, 22]. Recently, we have enabled a clinical infrastructure for advanced MRI investigations in patients presenting with acute ischemic unilateral LVO stroke after reperfusion therapy (IMPreST prospective cohort study, https://www.stroke.uzh.ch/en.html).

We therefore studied the presence of BOLD-CVR identified steal, i.e., a paradoxical BOLD signal drop during hypercapnia [19], and its association with diffusion-weighted imaging (DWI) lesions, as well as clinical outcome after acute ischemic unilateral LVO stroke following successful endovascular thrombectomy.

Materials and Methods

Study Population

From the prospective IMPreST (Interplay of Microcirculation and Plasticity after ischemic Stroke) longitudinal observational cohort study, we selected all patients with acute ischemic unilateral LVO stroke of the anterior circulation that were successfully treated with EVT (modified Thrombolysis In Cerebral Infarction—mTICI—scale ≥ 2b [23]) and received BOLD-CVR examination. The IMPreST study is a prospective study designed to explore the correlation between different imaging modalities for microcirculation and its association with clinical outcome in patients with acute ischemic unilateral LVO stroke. Inclusion criteria were: (1) ≤ 72 h first-ever clinical ischemic stroke at hospital admission; (2) occlusion of M1/M2-segment of the middle cerebral artery, and/or intracranial internal carotid artery, and perfusion deficits with cortical involvement; (3) 18 years or above; (4) living independent before stroke (modified Ranking Scale—mRS—≤ 3 [24]); (5) written informed consent of the patient or when the patient is not able to participate in the consenting procedure, the written authorization of an independent doctor who is not involved in the research project to safeguard the interests of the patients (in that case, post hoc written informed consent of the patient or next of kin had to be obtained). Exclusion criteria were the following: (1) major cardiac, psychiatric and/or neurological diseases; (2) early seizures; (3) known or suspected non-compliance, drug and/or alcohol abuse; (4) contra-indications for MRI; and (5) documented evidence that the patient does not want to participate in any scientific study. After EVT was evaluated and, eventually, conducted, the included patients received standard multimodality MRI at predefined time points (i.e., ≤ 72 h, at day 7 ± 3, at day 90 ± 14) from stroke symptom onset. The multimodal MR examination included 3D T1-MPRAGE, DWI, intravoxel incoherent motion (IVIM) imaging, susceptibility-weighted imaging (SWI), BOLD-CVR, 3D Time-Of-Flight (TOF) MR angiography, and 2D phase-contrast imaging using the 3D coordinates determined by non-invasive optimal vessel analysis (NOVA) software (VasSol Inc.), dynamic susceptibility contrast (DSC) MR perfusion. Given the objective of this work, we considered only BOLD-CVR and DWI data acquired in patients

successfully treated with EVT during the first examination session (i.e., ≤ 72 h from stroke symptom onset).

Ethics

The research ethic committee of the Canton Zurich, Switzerland (Kantonale Ethikkommission Zürich; KEK-ZH-NR. 2019–00750) approved the IMPreST prospective observational cohort study. Written informed consent was obtained from each participant before inclusion. The study was conducted in accordance with the ethical standards as laid down in the 1964 Declaration of Helsinki and its later amendments.

Image Acquisition Protocol

The imaging study was performed at 3-Tesla Skyra MRI scanner (Siemens Healthineers, Forchheim, Germany) with a 32-channel head matrix coil after the patients have been enrolled in the study. The exact scanning protocol of the investigated sequences — BOLD-CVR, DWI, 3D T1-MPRAGE — can be reviewed in the Supplementary information section.

During the BOLD MRI sequence, a standardized carbon dioxide (CO_2) stimulus was applied using the RespirAct™ (Thornhill Research Institute, Toronto, Canada), that allows for precise CO_2 end-tidal pressure ($P_{et}CO_2$) targeting while maintaining normal levels of O_2 (iso-oxia) [25]. Our standardized CO_2 protocol consisted of an initial 100 s at the patient-specific resting $P_{et}CO_2$, after which $P_{et}CO_2$ was increased to 10 mmHg for 80 s, and a return to resting $P_{et}CO_2$ for 120 s; $P_{et}O_2$ was maintained at the patient-specific resting value for the entire duration of the examination.

As specified above, BOLD-CVR imaging and DWI data were collected in a single examination session within 72 h from stroke symptom onset. The quality of the single BOLD-CVR imaging data was evaluated considering head motion artifacts and the consistency of the CO_2 stimulus. Specifically, examination were discarded from our analysis if the mean frame-wise displacement between adjacent acquisition volumes was > 2 mm [26] or if the CO_2 step change was < 6 mmHg.

Image Processing

Morphological and functional images were first processed singularly to calculate parameter maps. BOLD-CVR maps were obtained according to the previously described Zurich analysis pipeline [27] using MATLAB2019 (The MathWorks, Inc., Natrick, USA) and SPM12 (Wellcome Trust Centre for Neuroimaging, Institute of Neurology, University College London). BOLD-CVR was calculated voxel-per-voxel as percentage of BOLD signal change divided by the absolute change in $P_{et}CO_2$ (% ΔBOLD/ mmHg). Apparent diffusion coefficient (ADC) maps were automatically calculated from DWI data. All the resulting maps were then co-registered to the individual anatomical T1 space (intra-individual co-registration) using SPM12. Lastly, we extrapolated quantitative values from the co-registered parameter maps for different region of interests (ROIs) — i.e., whole brain (WB), grey matter (GM) and white matter (WM), ipsilateral and contralateral hemisphere, and major vascular territories (anterior cerebral artery, ACA; middle cerebral artery, MCA; posterior cerebral artery, PCA). ROIs of the vascular territories were provided by the recently published atlases by Liu et al. [28] To better investigate brain areas under steal, we selected for each patient the relevant voxels showing negative response in the BOLD-CVR map. First, we considered all voxels with < 0% BOLD signal change/mmHg CO_2. Then, using our healthy atlas as reference, a Z-score map [29] of the BOLD-CVR map was generated and the voxels with Z-score < 2 were excluded. In this way, only those negative voxels that differed significantly from the healthy cohort were considered (Supplementary Fig. 1). Additionally, for each patient, the deep learning-based algorithm by Liu et al. was used to automatically segment stroke lesion from DWI data (DWI infarct stroke lesion) [30].

Statistical Analysis

The statistical analysis of this study was carried out with the statistical program *R studio* (Posit Software, PBC formerly R Studio, version 02.07.2022). First, we described for each patient the mean BOLD-CVR values as well as the volumetric distribution of BOLD-CVR associated steal phenomenon in the different vascular territories and within the DWI infarct stroke lesion. Secondly, we looked at the spatial correlation between BOLD-CVR associated steal phenomenon and DWI infarct lesion by calculating the percentage of tissue exhibiting steal phenomenon that was also included in the infarct lesion. We defined therefore DWI-positive steal phenomenon-positive respectively DWI-negative steal phenomenon-positive brain tissue areas, and we performed a Spearman's correlation analysis to study the correlation between DWI-negative steal phenomenon-positive brain tissue and DWI infarct lesion. Groin Puncture-to-MR time (in hours, defined as time between start of EVT and first MR study session) and pre-EVT NIHSS were considered as covariates because we think that the first can be possible confounder correlating with steal phenomenon and DWI-lesion size and the second a surrogate of the extent of the initial penumbral tissue. Lastly, we modeled an ordinal logistic regression model [31–33] to study the effect of the presence of DWI-negative steal-positive brain

tissue on NIHSS values at discharge. We considered DWI lesion volumes as covariate because we think that this can be a possible confounder correlating with NIHSS values at discharge and steal phenomenon as well as age and pre-EVT NIHSS values as relevant baseline prognostic factors [34]. To check if the proportional odds assumption was satisfied, we used the Brant-Wald test.

Results

Between October 2019 and February 2022, twenty-six patients with acute ischemic unilateral LVO stroke consecutively included in the IMPreST prospective study received BOLD-CVR examination within 72 h from stroke symptom onset. Of these, 5 patients were excluded due to excessive head movement during MR examination. Twenty-one patients were included in analysis (Fig. 1) and their baseline characteristics can be reviewed in Table 1.

In the MR examination session after successful reperfusion therapy, we found high variability of the presence of steal phenomenon in the affected MCA and ACA territory of the included patients, with a median volume of 22 mL (IQR, 8–64). Table 2 summarizes the volumetric distribution of BOLD-CVR steal for all the included patients. Interestingly, steal-affected regions were heterogeneously distributed both within and outside the DWI lesion. On average, only 19% (INR, 8–59) of DWI lesion overlapped the steal area; respectively only 26% (IQR, 14–39) of steal volume was part of the DWI lesion (Supplementary Fig. 2). Within the DWI lesion, on average, severely impaired BOLD-CVR values were observed (mean ± SD; 0.042 ± 0.058 ΔBOLD%/mmHg). The comparison between DWI lesion size and steal phenomenon volume outside the DWI lesion can be reviewed in Fig. 2A. A Spearman's correlation analysis showed a positive partial correlation between DWI lesion volume and BOLD-CVR steal volume found outside the stroke lesion (correlation coefficient, r, 0.77; P value < 0.001). This correlation was maintained also after adjusting for Groin Puncture-to-MR time and pre-EVT NIHSS as confounding variables (r 0.76; P value < 0.001). The extent of steal phenomenon outside the DWI lesion did not show any significant dependency with respect to time from the start of EVT to the first MR examination session (r -0.20; P value 0.411) and pre-EVT NIHSS scale (r 0.36; P value 0.126).

Fig. 1 Study flow chart. LVO indicates large-vessel occlusion stroke; IMPreST, Interplay of Microcirculation and Plasticity after ischemic Stroke; EVT, endovascular thrombectomy; mTICI, modified Thrombolysis in Cerebral Infarction; MR, magnetic resonance; BOLD-CVR, blood oxygen level dependent cerebrovascular reactivity; DWI, diffusion-weighted imaging
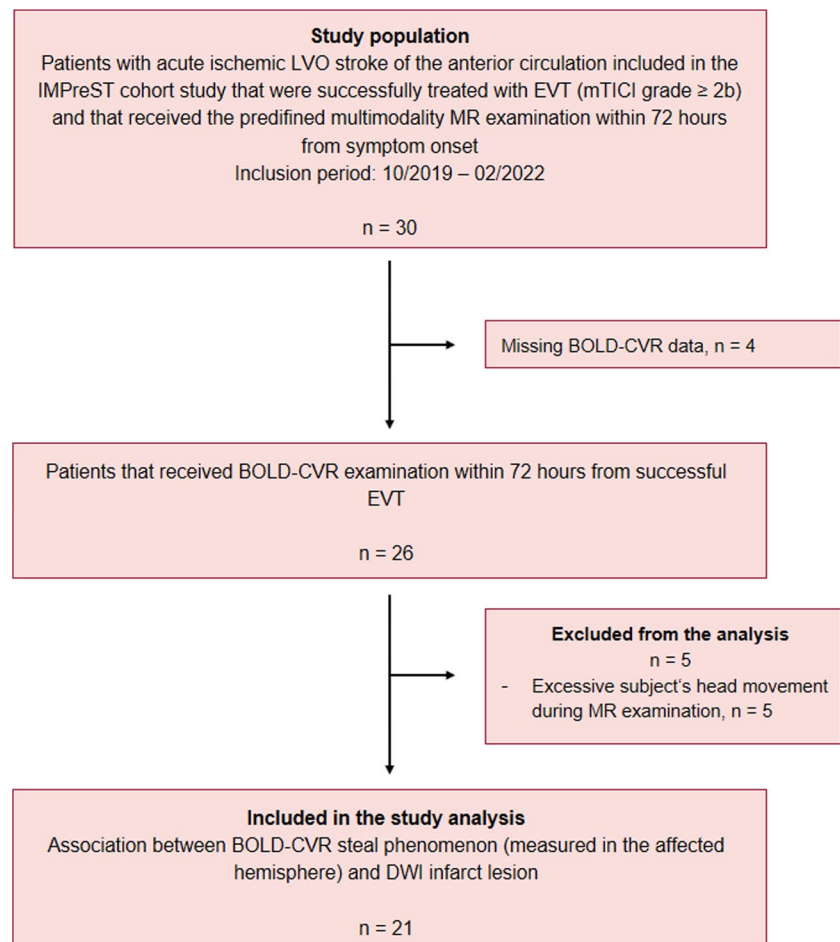
Table 1 Baseline characteristics

Baseline demographics	All ($n=21$)
Age	
Mean ± SD	69 ± 15
Year group	
< 50	3 (14%)
50–70	8 (38%)
> 70	10 (48%)
Sex	
M	9 (43%)
F	12 (57%)
Diseased vessel	
ICA	2 (10%)
MCA (M1/M2 segment)	11 (52%)
Both	8 (38%)
Clinical score at hospital admission	
NIHSS	
Median [IQR]	10.00 [8.00–16.00]
mRS	
Median [IQR]	4.00 [3.00–5.00]
Comorbidities	
Atrial fibrillation	4 (20%)
Smoking history	5 (24%)
Hypertension	13 (55%)
Dyslipidemia	8 (40%)
Obesity	3 (15%)
Diabetes	1 (5%)
Acute reperfusion therapy	
IVT	10 (50%)
EVT	21 (100%)
Symptom-to-needle time	
< 4.5 h	12 (57%)
> 4.5 h	2 (10%)
Wake-up stroke	7 (33%)
mTICI grade	
2b	5 (24%)
2c	3 (14%)
3	13 (62%)
Symptom-to-MR time	
< 24 h	3 (30%)
24–48 h	11 (40%)
48–72 h	7 (30%)
DWI infarct lesion [mL]	
Median [IQR]	26.30 [14.58–52.84]

ICA indicates internal carotid artery; *MCA*, middle carotid artery; *NIHSS*, National Institutes of Health Stroke Scale; *mRS*, modified Ranking Scale; *mTICI*, modified Thrombolysis in Cerebral Infarction; *IVT*, intravenous thrombolysis; *EVT*, endovascular thrombectomy; *MR*, magnetic resonance; *DWI*, diffusion-weighted imaging

At hospital discharge, the median NIHSS score value was 2 (IQR, 1–7). Fifteen patients had a NIHSS score equal or less than 3 (median, min–max; 1, 0–3), the remaining six patients more than 3 (median, min–max; 9, 7–18). The comparison of NIHSS at hospital discharge and DWI lesion size as well as steal phenomenon volumes outside the DWI lesion are presented in Fig. 2B.

Unadjusted ordinal regression analysis showed that the volume of BOLD-CVR defined steal found outside the DWI lesion was significantly associated with NIHSS score at discharge (regression coefficient 0.053; 95%-CI 0.023 to 0.092; *P* value 0.002). After adjusting for DWI lesion size, pre-EVT NIHSS values, and age the trend of the association was maintained but was not significant (Table 3), most likely due to the small sample size. In Fig. 3, BOLD-CVR and DWI findings of four example patients are presented.

Discussion

Our study shows that BOLD-CVR associated steal phenomenon can be detected in the affected hemisphere of patients with acute ischemic unilateral LVO stroke despite successful EVT, which reflects microcirculatory autoregulatory impairment and may therefore indicate reperfusion failure. Brain areas with steal phenomenon only showed a partial spatial agreement with DWI infarct lesions, whereas steal phenomenon was also observed in brain tissue outside the DWI lesion. The brain tissue volume exhibiting steal phenomenon outside the infarct — DWI — lesion correlated strongly with the volume of DWI derived infarct lesion and was a significant predictor for a poorer clinical status at hospital discharge.

To the best of our knowledge, we could not identify similar studies measuring CVR after acute reperfusion therapy in a similar cohort of patients, and therefore a direct comparison of our results with already existing findings is not possible to date. However, some clinical studies reported the findings observed with other imaging techniques [35–39]. A dynamic growth of DWI lesion after revascularization procedures has been observed reflecting reperfusion failure [35, 39]. Infarct growth contributes to the final infarct volume, correlates with clinical outcome and has been associated with DWI lesion size pre-EVT as well as mTICI grade < 2b and hypoperfusion post-EVT [35]. These findings enhance the importance of identifying prognostic factors that are associated with reperfusion failure and can therefore predict infarct lesion evolution after EVT. A recent work of Potreck et al. [37] studied tissue response after successful EVT with combined perfusion and permeability MR imaging and showed distinct post-reperfusion pathophysiological tissue responses that were associated with different clinical courses. In general,

Table 2 Distribution of BOLD-CVR associated steal phenomenon in the affected hemisphere

Subject	Mean BOLD-CVR in MCA territory	Mean BOLD-CVR in ACA territory	Mean ± SD BOLD-CVR in DWI lesion	DWI infarct lesion volume	SP volume in ACA + MCA territory	SP volume in DWI lesion	SP volume outside DWI lesion
1	0.07	0.11	0.04 ± 0.01	10.18	14.94	3.84	11.09
2	0.09	0.07	0.02 ± 0.01	14.58	42.64	6.42	36.22
3	0.08	0.14	0.06 ± 0.01	47.15	4.40	0.70	3.70
4	0.11	0.09	0.08 ± 0.01	2.02	2.71	0.06	2.65
5	0.06	0.08	0.01 ± 0.01	97.12	189.76	73.84	115.92
6	− 0.03	− 0.01	− 0.03 ± 0.02	117.29	174.03	73.75	100.28
7	0.08	0.06	− 0.03 ± 0.02	72.13	129.37	45.88	83.49
8	0.08	0.06	0.06 ± 0.01	26.30	8.77	1.24	7.54
9	0.12	0.08	0.04 ± 0.01	13.89	4.07	1.34	2.73
10	0.14	0.12	0.08 ± 0.01	4.29	2.59	0.00	2.60
11	0.19	0.23	0.09 ± 0.02	18.00	21.58	2.79	18.78
12	0.15	0.20	0.03 ± 0.03	36.41	42.69	19.34	23.35
13	0.08	0.08	− 0.01 ± 0.01	89.57	83.99	51.79	32.20
14	0.06	0.00	0.03 ± 0.01	17.74	25.79	3.28	22.51
15	0.20	0.14	0.17 ± 0.02	1.33	0.36	0.00	0.36
16	0.06	0.15	− 0.05 ± 0.01	52.84	113.19	46.55	66.64
17	0.04	0.05	− 0.04 ± 0.02	23.30	57.50	17.92	39.57
18	0.13	0.10	0.08 ± 0.01	30.78	18.49	4.97	13.52
19	0.18	0.13	0.13 ± 0.02	16.18	9.51	2.11	7.40
20	0.11	0.10	0.05 ± 0.01	80.20	33.94	21.05	12.89
21	0.14	0.12	0.08 ± 0.01	30.30	4.08	0.59	3.49

BOLD-CVR values are reported with unit [% ΔBOLD/mmHg]; volumes are reported with unit [mL]; BOLD-CVR indicates blood oxygen level dependent cerebrovascular reactivity; *SP*, steal phenomenon; *GM*, grey matter; *WM*, white matter; *ACA*, anterior cerebral artery; *MCA*, middle cerebral artery; *PCA*, posterior cerebral artery

hypoperfusion occurred more often in patients with unfavourable clinical outcome compared to hyperperfusion or unchanged perfusion. BOLD-CVR imaging, thanks to its capability to study vessel reactivity, offers the potential to provide additional information about microvascular functionality. We focused our analysis on brain regions exhibiting BOLD-CVR identified steal because we thought this could represent irreversible tissue damage and/or brain areas subjected to reperfusion failure. Based on the current knowledge on the pathophysiological mechanisms of reperfusion failure [9, 14, 16], we hypothesized that steal phenomenon could reflect on of the following: (1) exhausted regional vasodilatory reserve induced by microvascular occlusion with microclots, microvascular occlusion with recruited neutrophils, and/or vessel constriction; (2) loss of cerebrovascular autoregulation. Most of the knowledge about reperfusion failure mechanisms came from pre-clinical studies. Recently, Binder et al. [40] investigated the role of leptomeningeal collaterals in reperfusion failure in a rodent stroke model and reported a loss of vascular tone (i.e., loss of autoregulation) in the distal MCA branch segments after reperfusion which was associated with a worse clinical outcome.

In our study, we observed a partial spatial agreement between DWI infarct lesion and BOLD-CVR identified steal. We can distinguish three different tissue areas: DWI-positive steal-negative brain tissue, DWI-positive steal-positive brain tissue, and DWI-negative steal-positive brain tissue. In the DWI infarct lesion ("DWI-positive"), both steal phenomenon and impaired, but maintained BOLD-CVR values were observed. A possible explanation to this finding is that two different tissue classes can be present in the DWI lesion: (1) infarcted necrotic tissue with disrupted vessels (i.e., no cerebrovascular reactivity) that consequently shows BOLD-CVR around zero with either slightly positive or slightly negative values [41]; (2) tissue not yet irreversible damaged that shows maintained cerebrovascular reactivity after successful reperfusion [39, 42]. Of major clinical relevance, we observed tissue exhibiting a steal phenomenon that was not included in the DWI lesion ("DWI-negative"), which could indicate tissue not irreversibly damaged but with severely impaired hemodynamic characteristics. We found a positive correlation of this DWI-negative steal-positive brain tissue with DWI infarct lesion size and a significant association with higher NIHSS clinical score at hospital discharge. These
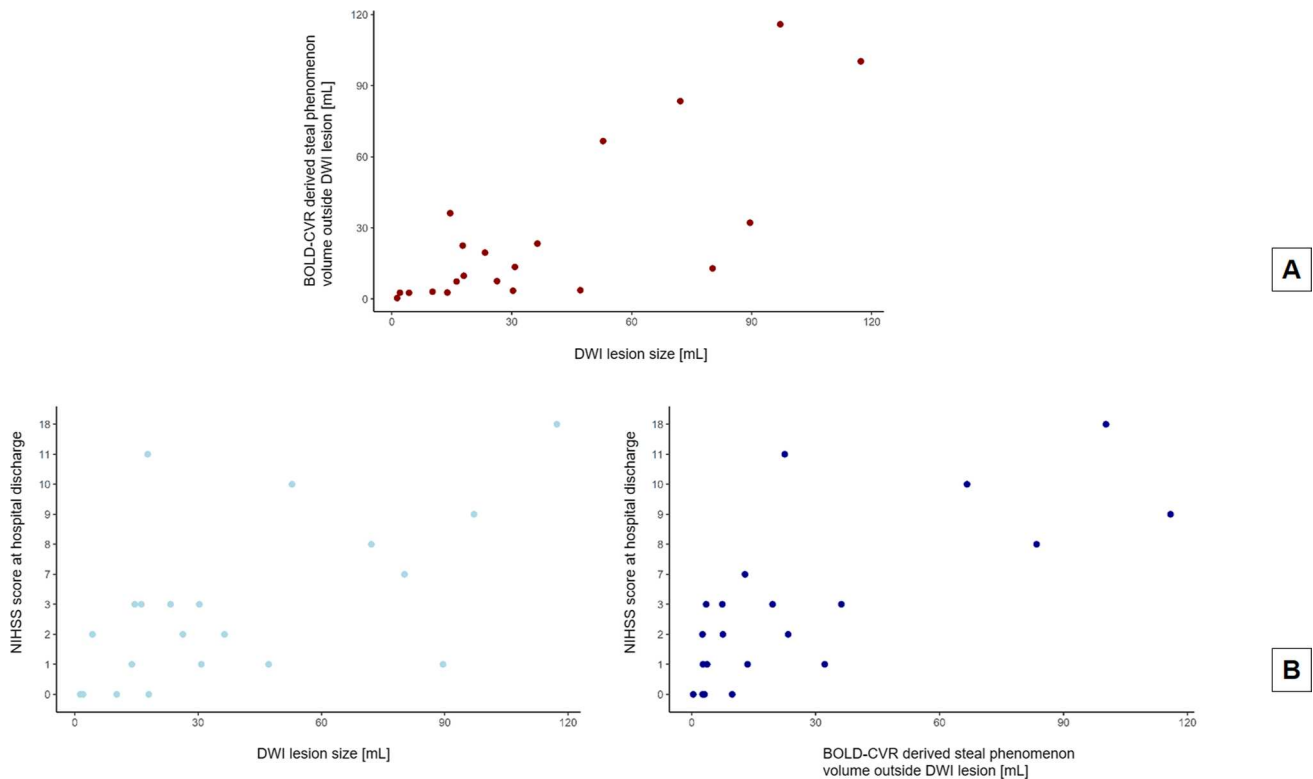
Fig. 2 Comparison plots. Panel A shows the comparison of DWI lesion size with BOLD-CVR derived steal phenomenon volume outside the DWI lesion. Panel B shows the comparison of DWI lesion size, respectively BOLD-CVR derived steal phenomenon volume outside the DWI lesion, with the NIHSS score at hospital discharge. DWI indicates diffusion-weighted imaging; BOLD-CVR, blood oxygen level dependent cerebrovascular reactivity; NIHSS, National Institutes of Health Stroke Scale

Table 3 Results of the linear regression model of the association between BOLD-CVR associated steal phenomenon volume outside the infarct lesion and NIHSS score value at hospital discharge

Variable	β	95% confidence interval (95-CI)	P value
Age	−0.06	−0.14 to 0.01	0.086
BOLD-CVR associated SP outside the infarct lesion (mL)	0.04	0.00 to 0.10	0.066
DWI infarct lesion volume (mL)	0.02	−0.02 to 0.06	0.282
NIHSS at hospital admission	0.17	−0.02 to 0.37	0.089

β indicates the regression coefficient; *BOLD-CVR*, blood oxygen level dependent cerebrovascular reactivity; *SP*, steal phenomenon; *DWI*, diffusion-weighted imaging; *NIHSS*, National Institutes of Health Stroke Scale

findings indirectly support what we assumed in the beginning, namely, that the steal phenomenon does not reflect just infarcted tissue and that the identified DWI-negative steal-positive region could depict brain tissue with microvascular dysfunction (i.e., reperfusion failure) that could evolve to an irreversibly infarcted area.

Future Directions

Our preliminary findings highlight the potential of BOLD-CVR imaging as a novel technique to characterize brain tissue hemodynamic responses after EVT. Future research, however, is needed to further understand the link between the observed BOLD-CVR steal phenomenon, reperfusion failure and its association with clinical outcome. These results need to be validated in a bigger study cohort and the clinical relevance of post-EVT BOLD-CVR findings on mid-term (90 days) and long-term clinical outcome (1 year) should also be investigated. A correlation analysis between BOLD-CVR findings and MR perfusion parameters (i.e., cerebral blood flow, CBF, cerebral blood volume, CBV, mean transit time, MTT, time-to-maximum, Tmax) could be performed to confirm our hypothesis of the mechanisms behind steal phenomenon observed in reperfused tissue (i.e., both loss of autoregulation with associated hyperperfusion and microvascular occlusion/constriction with associated hypoperfusion). In addition, a retrospective analysis to identify which pre-EVT clinical/imaging factors are associated with the occurrence of steal phenomenon could be considered.
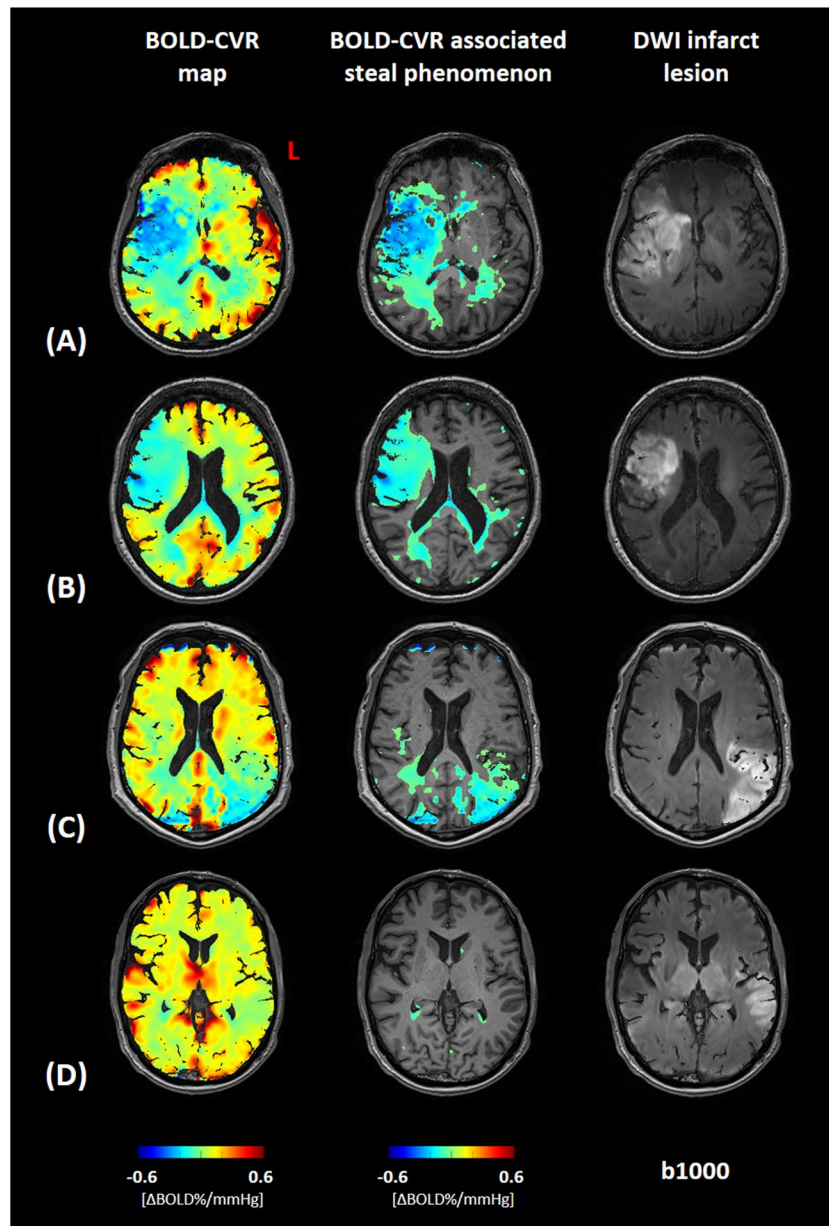
Fig. 3 Association between BOLD-CVR associated steal phenomenon and DWI infarct lesion. Blood oxygen level dependent cerebrovascular reactivity (BOLD-CVR) and trace DWI (diffusion-weighted imaging) map of four illustrative examples are presented. For each patient a whole-brain BOLD-CVR map, a BOLD-CVR showing only steal phenomenon tissue areas, and trace DWI map are depicted. (**A**) male subject (age range: 66–70 years) showing 97 mL infarct lesion in the middle cerebral artery (MCA) territory right, showing a total of 190 mL steal phenomenon, 74 mL within and 116 mL outside the infarct lesion. NIHSS 16 at hospital admission, NIHSS 9 at hospital discharge. (**B**) Female subject (age range: 66–70 years) show- ing 53 mL infarct lesion in the MCA territory right, showing a total of 113 mL steal phenomenon, 47 mL within and 67 mL outside the infarct lesion. NIHSS 12 at hospital admission, NIHSS 10 at hospital discharge. (**C**) Male subject (age range: 71–75 years) show- ing 90 mL infarct lesion in the MCA territory left, showing a total of 84 mL steal phenomenon, 52 mL within and 32 mL outside the infarct lesion. NIHSS 10 at hospital admission, NIHSS 1 at hospital discharge. (**D**) Male subject (age range: 66–70 years) showing 47 mL infarct lesion in the MCA territory left, showing a total of 4 mL steal phenomenon, 1 mL within and 4 mL outside the infarct lesion. NIHSS 3 at hospital admission, NIHSS 1 at hospital discharge

Strength and Limitations

This work represents a preliminary analysis of BOLD-CVR findings in a well-defined cohort of patients with acute ischemic unilateral LVO stroke. The investigated imaging modalities (BOLD-CVR and DWI) were acquired within the same examination session and therefore high intra-subject comparability between imaging data can be

assumed. However, this study has some limitations. First, the small sample size of the studied cohort limited the statistical power as well as the generalizability of our analysis and therefore further studies including more patients are necessary to confirm our observations. Second, to avoid unethical diagnostic delay, our study did not provide imaging data about tissue state before reperfusion therapy. Therefore, the clinical meaning of BOLD-CVR identified steal before EVT is unknown. Third, we created a steal phenomenon mask from the BOLD-CVR magnitude maps selecting all the voxel exhibiting a negative response to the hypercapnic stimulus. However, the clinical relevance of this steal phenomenon mask has not yet been investigated and other definitions based on different thresholds respectively considering also more technical imaging aspects (e.g., contrast-to-noise ratio) should be also evaluated in the future.

Conclusions

Patients with unilateral acute ischemic large-vessel occlusion stroke exhibit BOLD-CVR associated steal in the early phase despite successful EVT. Steal volume was associated with DWI lesion size, and with poor clinical outcome at hospital discharge. The BOLD-CVR identified steal phenomenon may provide a better understanding of persisting hemodynamic impairment following reperfusion therapy.

Declarations

Competing interests The authors declare no competing interests.

References

1. Muir KW, Buchan A, von Kummer R, Rother J, Baron JC. Imaging of acute stroke. Lancet Neurol. 2006;5(9):755–68. https://doi.org/10.1016/S1474-4422(06)70545-2.

2. Seifert K, Heit JJ. Collateral blood flow and ischemic core growth. Transl Stroke Res. 2023;14(1):13–21. https://doi.org/10.1007/s12975-022-01051-2.

3. Seners P, Yuen N, Mlynash M, Snyder SJ, et al. Quantification of penumbral volume in association with time from stroke onset in acute ischemic stroke with large vessel occlusion. JAMA Neurol. 2023;80(5):523. https://doi.org/10.1001/jamaneurol.2023.0265.

4. Sebök M, Esposito G, Van Niftrik CHB, et al. Flow augmentation STA-MCA bypass evaluation for patients with acute stroke and unilateral large vessel occlusion: a proposal for an urgent bypass flowchart. J Neurosurg. 2022;137(4):1047–55. https://doi.org/10.3171/2021.10.jns21986.

5. Powers WJ, Rabinstein AA, Ackerson T, et al. Guidelines for the early management of patients with acute ischemic stroke: 2019 update to the 2018 guidelines for the early management of acute ischemic stroke: a guideline for healthcare professionals from the American Heart Association/American Stroke Association. Stroke. 2019;50(12):e344–418. https://doi.org/10.1161/STR.0000000000000211.

6. Hankey GJ. Stroke. Lancet Lond Engl. 2017;389(10069):641–54. https://doi.org/10.1016/S0140-6736(16)30962-X.

7. Malik P, Anwar A, Patel R, Patel U. Expansion of the dimensions in the current management of acute ischemic stroke. J Neurol. 2021;268(9):3185–202. https://doi.org/10.1007/s00415-020-09873-6.

8. Olthuis SGH, Pirson A, Pinckaers FME, et al. Endovascular treatment versus no endovascular treatment after 6–24 h in patients with ischaemic stroke and collateral flow on CT angiography (MR CLEAN-LATE) in the Netherlands: a multicentre, open-label, blinded-endpoint, randomised, controlled, phase 3 trial. The Lancet. 2023;401(10385):1371–80. https://doi.org/10.1016/S0140-6736(23)00575-5.

9. El Amki M, Wegener S. Improving cerebral blood flow after arterial recanalization: a novel therapeutic strategy in stroke. Int J Mol Sci. 2017;18(12):2669. https://doi.org/10.3390/ijms18122669.

10. Nie X, Leng X, Miao Z, Fisher M, Liu L. Clinically ineffective reperfusion after endovascular therapy in acute ischemic stroke. Stroke. 2023;54(3):873–81. https://doi.org/10.1161/STROKEAHA.122.038466.

11. Lee JS, Bang OY. Collateral status and outcomes after thrombectomy. Transl Stroke Res. 2023;14(1):22–37. https://doi.org/10.1007/s12975-022-01046-z.

12. Zhang Z, Pu Y, Mi D, Liu L. Cerebral hemodynamic evaluation after cerebral recanalization therapy for acute ischemic stroke.

Front Neurol. 2019;10:719. https://doi.org/10.3389/fneur.2019.00719.

13. Van Der Knaap, N., Franx, B. a. A., Majoie, C. B. L. M., et al. Implications of Post-recanalization Perfusion Deficit After Acute Ischemic Stroke: a Scoping Review of Clinical and Preclinical Imaging Studies. Translational Stroke Research, 2023. https://doi.org/10.1007/s12975-022-01120-6.

14. Okada Y, Copeland BR, Fitridge R, Koziol JA, del Zoppo GJ. Fibrin contributes to microvascular obstructions and parenchymal changes during early focal cerebral ischemia and reperfusion. Stroke. 1994;25(9):1847–53. https://doi.org/10.1161/01.str.25.9.1847. (discussion 1853-1854).

15. El Amki M, Glück C, Binder N, et al. Neutrophils obstructing brain capillaries are a major cause of no-reflow in ischemic stroke. Cell Rep. 2020;33(2):108260. https://doi.org/10.1016/j.celrep.2020.108260.

16. Rayasam A, Hsu M, Kijak JA, et al. Immune responses in stroke: how the immune system contributes to damage and healing after stroke and how this knowledge could be translated to better cures? Immunology. 2018;154(3):363–76. https://doi.org/10.1111/imm.12918.

17. Lin YH, Liu HM. Update on cerebral hyperperfusion syndrome. J Neurointerventional Surg. 2020;12(8):788–93. https://doi.org/10.1136/neurintsurg-2019-015621.

18. Fisher JA, Venkatraghavan L, Mikulis DJ. Magnetic resonance imaging-based cerebrovascular reactivity and hemodynamic reserve. Stroke. 2018;49(8):2011–8. https://doi.org/10.1161/STROKEAHA.118.021012.

19. Sobczyk O, Battisti-Charbonney A, Fierstra J, et al. A conceptual model for CO2-induced redistribution of cerebral blood flow with experimental confirmation using BOLD MRI. Neuroimage. 2014;92:56–68. https://doi.org/10.1016/j.neuroimage.2014.01.051.

20. Fierstra J, Sobczyk O, Battisti-Charbonney A, et al. Measuring cerebrovascular reactivity: what stimulus to use? J Physiol. 2013;591(23):5809–21. https://doi.org/10.1113/jphysiol.2013.259150.

21. van Niftrik CHB, Sebök M, Wegener S, et al. Increased ipsilateral posterior cerebral artery P2-segment flow velocity predicts hemodynamic impairment. Stroke. 2021;52(4):1469–72. https://doi.org/10.1161/STROKEAHA.120.032848.

22. Sebök M, van Niftrik CHB, Lohaus N, et al. Leptomeningeal collateral activation indicates severely impaired cerebrovascular reserve capacity in patients with symptomatic unilateral carotid artery occlusion. J Cereb Blood Flow Metab Off J Int Soc Cereb Blood Flow Metab. 2021;41(11):3039–51. https://doi.org/10.1177/0271678X211024373.

23. Zaidat OO, Yoo AJ, Khatri P, et al. Recommendations on angiographic revascularization grading standards for acute ischemic stroke: a consensus statement. Stroke. 2013;44(9):2650–63. https://doi.org/10.1161/STROKEAHA.113.001972.

24. Rankin J. Cerebral vascular accidents in patients over the age of 60. II. Prognosis. Scott Med J. 1957;2(5):200–15. https://doi.org/10.1177/003693305700200504.

25. Slessarev M, Han J, Mardimae A, et al. Prospective targeting and control of end-tidal CO2 and O2 concentrations. J Physiol. 2007;581(3):1207–19. https://doi.org/10.1113/jphysiol.2007.129395.

26. Power JD, Mitra A, Laumann TO, Snyder AZ, Schlaggar BL, Petersen SE. Methods to detect, characterize, and remove motion artifact in resting state fMRI. Neuroimage. 2014;84:320–41. https://doi.org/10.1016/j.neuroimage.2013.08.048.

27. van Niftrik CHB, Piccirelli M, Bozinov O, et al. Iterative analysis of cerebrovascular reactivity dynamic response by temporal decomposition. Brain Behav. 2017;7(9):e00705. https://doi.org/10.1002/brb3.705.

28. Liu CF, Hsu J, Xu X, et al. Digital 3D brain MRI arterial territories atlas. Sci Data. 2023;10(1):74. https://doi.org/10.1038/s41597-022-01923-0.

29. Sobczyk O, Battisti-Charbonney A, Poublanc J, et al. Assessing cerebrovascular reactivity abnormality by comparison to a reference atlas. J Cereb Blood Flow Metab Off J Int Soc Cereb Blood Flow Metab. 2015;35(2):213–20. https://doi.org/10.1038/jcbfm.2014.184.

30. Liu CF, Hsu J, Xu X, et al. Deep learning-based detection and segmentation of diffusion abnormalities in acute ischemic stroke. Commun Med. 2021;1:61. https://doi.org/10.1038/s43856-021-00062-8.

31. Winship C, Mare RD. Regression models with ordinal variables. Am Sociol Rev. 1984;49(4):512. https://doi.org/10.2307/2095465.

32. Haubo, R. Cumulative Link Models for Ordinal Regression with the R Package ordinal. 2018. https://www.semanticscholar.org/paper/Cumulative-Link-Models-for-Ordinal-Regression-with-Haubo-Christensen/2130d63b9a6eab9612b97b0b738122a30d636227

33. Optimising Analysis of Stroke Trials (OAST) collaboration, Bath PMW, Gray LJ, Collier T, Pocock S, Carpenter J. Can we improve the statistical analysis of stroke trials? Statistical reanalysis of functional outcomes in stroke trials. Stroke. 2007;38(6):1911–5. https://doi.org/10.1161/STROKEAHA.106.474080.

34. Optimising Analysis of Stroke Trials (OAST) Collaboration. Should stroke trials adjust functional outcome for baseline prognostic factors? Stroke. 2009;40(3):888–94. https://doi.org/10.1161/STROKEAHA.108.519207.

35. Hernández-Pérez M, Werner M, Friedemann SR, et al. Early and delayed infarct growth in patients undergoing mechanical thrombectomy: A Prospective. Serial MRI study Stroke. 2023;54(1):217–25. https://doi.org/10.1161/strokeaha.122.039090.

36. Kosior JC, Buck B, Wannamaker R, et al. Exploring reperfusion following endovascular thrombectomy. Stroke. 2019;50(9):2389–95. https://doi.org/10.1161/STROKEAHA.119.025537.

37. Potreck A, Mutke MA, Weyland CS, et al. Combined perfusion and permeability imaging reveals different pathophysiologic tissue responses after successful thrombectomy. Transl Stroke Res. 2021;12(5):799–807. https://doi.org/10.1007/s12975-020-00885-y.

38. Gwak DS, Choi W, Shim DH, et al. Role of apparent diffusion coefficient gradient within diffusion lesions in outcomes of large stroke after thrombectomy. Stroke. 2022;53(3):921–9. https://doi.org/10.1161/STROKEAHA.121.035615.

39. Nagaraja N, Forder JR, Warach S, Merino JG. Reversible diffusion-weighted imaging lesions in acute ischemic stroke: a systematic review. Neurology. 2020;94(13):571–87. https://doi.org/10.1212/WNL.0000000000009173.

40. Binder NF, El Amki M, Glück C, et al. Leptomeningeal collaterals regulate reperfusion in ischemic stroke. bioRxiv. 2023;02.25.529915. https://doi.org/10.1101/2023.02.25.529915. This article is a preprint and has not been certified by peer review.

41. Garcia JH. The neuropathology of stroke. Hum Pathol. 1975;6(5):583–98. https://doi.org/10.1016/s0046-8177(75)80043-8.

42. Goyal M, Ospel JM, Menon B, et al. Challenging the ischemic core concept in acute ischemic stroke imaging. Stroke. 2020;51(10):3147–55. https://doi.org/10.1161/STROKEAHA.120.030620.